Effective wave propagation modelling in subsurface offshore geological structures with time sub-cycling FEM procedures

Lucas Ruffo Pinto[1], Delfim Soares Jr.[2], Webe João Mansur[1]
[1]COPPE / Federal University of Rio de Janeiro, [2]Structural Engineering Department / Federal University of Juiz de Fora

This paper was prepared for presentation during the 17th International Congress of the Brazilian Geophysical Society held in Rio de Janeiro, Brazil, 16-19 August 2021.

Abstract

This work presents two explicit methodologies considering adaptive time integrators, applied together with techniques of domain subdivision and sub-cycling, for time domain analyses of elastodynamic models. The methods are accurate, providing reduced period elongation and/or amplitude decay errors, and they allow introducing adaptive numerical dissipation of spurious oscillations. Since the techniques are explicit, they do not need to consider any solver routine, standing as very efficient methodologies. The discussed α explicit adaptive method has the same stability limit as the central difference method (CDM), while the β explicit adaptive method has an improved stability limit, whose value may be up to twice that of the CDM. Subdomain decomposition procedures, associated to multiple time-steps and sub-cycling, are also considered herein to improve the performance of the formulation. Thereby, it is possible to consider higher time-step values in the analyses, providing lower computational costs. In addition, this approach allows the elements of the spatially discretized model to march closer to their stability limits, improving the accuracy of the analysis. At the end of the paper, numerical results are presented in comparison to those of the CDM and the explicit generalized α method (EG-α), illustrating the effectiveness of the discussed approaches.

Introduction

Time dependent hyperbolic equations have numerous applications in science and engineering development, as they make it possible to describe time dependent continuous domain physical problems. Nevertheless, they are challenging to be solved and their analytical resolution is often unfeasible. Therefore, in order to solve these equations, numerical methods are commonly used to find approximate solutions. These methods usually employ step-by-step time integration algorithms, solving initial value problems considering a temporal discretization. Numerical methods are basically divided into two groups: explicit methods [1-9], whose main advantage is that there is no need to deal with algorithms for solving systems of equations, making them computationally effective, yet with stability restrictions; and implicit methods [9-15], which provide unconditional stability, but are considerably more computationally expensive per time step (for a comprehensive review, see [16]).

In this paper, two explicit formulations with adaptive time integrators are studied, considering the implementation of sub-cycling techniques to improve the efficiency and accuracy of the proposed time integration algorithms. The explicit methods developed by Soares [1,9] give the following characteristics: (i) they are truly self-starting; (ii) based on single-step displacement-velocity relations; (iii) allow adaptive algorithmic dissipation; and, (iv) as explicit approaches, do not need to consider any solver routine. The α explicit adaptive (α-adap) method presents the same stability limit as the CDM; and the β explicit adaptive (β-adap) method has an improved stability limit, whose value may be up to twice that of the CDM (the β-adap method provides reduced period elongation errors as well). In addition, subdomain divisions and local time-step values are considered in this work, also taking into account automated adaptive evaluations. Thus, more efficient and accurate analysis may be enabled.

The adopted time integration procedures are based on adaptive parameters that focus on providing effective numerically dissipative algorithms, aiming to eliminate the influence of spurious high frequency modes and to reduce amplitude decay errors. In this sense, the time integrators (α or β) are adaptively computed taking into account the maximum sampling frequency of the elements, and the local time-step value. For the activation of the adaptive parameters, the results of the previous local time steps are considered. Thus, by introducing different time-steps into the analysis (considering subdomain divisions and sub-cycling techniques), the performance of the methodologies may be enhanced.

The techniques discussed in this work can be used to solve problems of different nature, however, here, elastodynamic analyses and geophysical applications are focused. In geophysics, it is often necessary to directly analyze very heterogeneous domains that feature several layers of different materials. In this sense, automatic sub-cycling techniques become very attractive, since these different layers/media may be efficiently analyzed considering proper subdomain divisions.

Governing equations and time integration strategies

The governing system of equations describing a dynamic model is given by:

$$\mathbf{M}\ddot{\mathbf{U}}(\mathrm{t}) + \mathbf{C}\dot{\mathbf{U}}(\mathrm{t}) + \mathbf{K}\mathbf{U}(\mathrm{t}) = \mathbf{F}(\mathrm{t}) \quad (1)$$

where $\mathbf{M}$, $\mathbf{C}$, and $\mathbf{K}$ stand for the mass, damping, and stiffness matrices, respectively; $\ddot{\mathbf{U}}(\mathrm{t})$, $\dot{\mathbf{U}}(\mathrm{t})$ and $\mathbf{U}(\mathrm{t})$ are acceleration, velocity, and displacement vectors, respectively; and $\mathbf{F}(\mathrm{t})$ stands for the force vector. The initial conditions of the model are given by: $\mathbf{U}^0 = \mathbf{U}(0)$ and $\dot{\mathbf{U}}^0 = \dot{\mathbf{U}}(0)$, where $\mathbf{U}^0$ and $\dot{\mathbf{U}}^0$ stand for initial displacement and velocity vectors, respectively.

The Finite Element Method (FEM) is used for the spatial discretization, since geological problems take great advantage of its ability to work with irregular geometries. By considering the standard FEM, the domain of the problem is divided into elements, allowing the calculation of local matrices and vectors, which can then be assembled to generate the global matrices $\mathbf{M}$, $\mathbf{C}$, and $\mathbf{K}$, and vector $\mathbf{F}$.

α - Explicit Adaptive Method

In this time-marching procedure, the displacements and velocities of the model are computed as follows:

$$\left(\mathbf{M}_e + \frac{1}{2}\Delta t\mathbf{C}_e\right)\dot{\mathbf{U}}_e^{n+1} = \int_{t^n}^{t^{n+1}} \mathbf{F}_e(t)\,dt + \mathbf{M}_e\dot{\mathbf{U}}_e^n - \frac{1}{2}\Delta t\mathbf{C}_e\dot{\mathbf{U}}_e^n - \mathbf{K}_e\left(\Delta t\mathbf{U}_e^n + \frac{1}{2}\alpha_e^n\Delta t^2\dot{\mathbf{U}}_e^n\right) \quad (2a)$$

$$\mathbf{U}^{n+1} = \mathbf{U}^n + \frac{1}{2}\Delta t\dot{\mathbf{U}}^n + \frac{1}{2}\Delta t\dot{\mathbf{U}}^{n+1} \quad (2b)$$

where Δt represents the time-step, and $\mathbf{U}^n$ and $\dot{\mathbf{U}}^n$ are the approximations of $\mathbf{U}(t^n)$ and $\dot{\mathbf{U}}(t^n)$, respectively. In eq. (2a), the subscript e indicates that a variable is locally defined, at an element level. Once eq. (2a) is assembled, the velocities of the model can be computed, and the displacements can then be evaluated following eq. (2b).

Considering the α parameter (see eq. (2a)), which controls numerical damping, the strategy is to adopt $\alpha > 1$ wherever and whenever numerical damping may be necessary, and $\alpha = 1$ otherwise. This is automatically carried out here based on an oscillatory criterion controlled by an φ parameter, that is calculated at each time step and for each element. The calculation of this oscillatory parameter is given by: $\varphi_e^n = \Sigma_{i=1}^{d_e} \left|\left|u_i^n - u_i^{n-2}\right| - \left|u_i^n - u_i^{n-1}\right| - \left|u_i^{n-1} - u_i^{n-2}\right|\right|$, where d_e stands for the total amount of degrees of freedom of the element. Therefore, when $\varphi \neq 0$, at least one degree of freedom of the element is oscillating. Thus, the algorithm activates maximal numerical dissipation at the maximal sampling frequency of the element Ω_e^{max}, effectively dissipating the highest modes of the problem. So, when $\varphi_e^n \neq 0$, α_e^n assumes the following value:

$$\alpha_e^{act} = (-\Omega_e^{max} - 4\zeta_e + 4(\Omega_e^{max}\zeta_e + 1)^{1/2})/\Omega_e^{max} \quad (3)$$

where $\zeta_e = \varsigma_e/(2\rho_e\omega_e^{max})$, and ω_e^{max}, ρ_e and ς_e stand for physical properties of the medium (maximum natural frequency, mass density and viscous damping coefficient, respectively). For $\varphi_e^n = 0$, $\alpha_e^n = 1$ is considered.

β - Explicit Adaptive Method

In this time-marching procedure, the displacements and velocities of the model are computed as follows:

$$\left(\mathbf{M} + \frac{1}{2}\Delta t\mathbf{C}\right)\dot{\mathbf{U}}^{n+1} = \int_{t^n}^{t^{n+1}} \mathbf{F}(t)\,dt + \mathbf{M}\dot{\mathbf{U}}^n - \frac{1}{2}\Delta t\mathbf{C}\dot{\mathbf{U}}^n - \mathbf{K}\left(\Delta t\mathbf{U}^n + \frac{1}{2}\Delta t^2\dot{\mathbf{U}}^n\right) \quad (4a)$$

$$\mathbf{U}^{n+1} = \mathbf{U}^n + \frac{1}{2}\Delta t\dot{\mathbf{U}}^n + \frac{1}{2}\Delta t\dot{\mathbf{U}}^{n+1} + \frac{1}{2}\Delta t\mathbf{V}^{n+1} \quad (4b)$$

where an additional $\mathbf{V}^{n+1}$ term is introduced into the formulation for the displacements, allowing to obtain greater stability limits for the explicit analysis. The vector $\mathbf{V}^{n+1}$ is given as follows:

$$\left(\mathbf{M}_e + \frac{1}{2}\Delta t\mathbf{C}_e\right)\mathbf{V}_e^{n+1} = -\Delta t\mathbf{C}_e\dot{\mathbf{U}}_e^{n+1} - \frac{1}{8}\Delta t^2\mathbf{K}_e\left((\beta_e^n)^2\dot{\mathbf{U}}_e^n + (1+\beta_e^n)\dot{\mathbf{U}}_e^{n+1}\right) \quad (5)$$

where, analogously to α_e^n, the β_e^n represents an integration parameter whose value varies for each element and for each time step of the analysis, controlling the dissipative properties of the technique. The strategy adopted for β is similar to that for α, i.e., $\beta > 0$ is applied wherever and whenever numerical damping may be necessary, and $\beta = 0$ otherwise. The parameter φ is also used to control the activation of numerical dissipation. So, when $\varphi_e^n \neq 0$, β_e^n assumes the following value:

$$\begin{aligned}\beta_e^{act} = (&-\Omega_e^{max^5} + 16\Omega_e^{max^3} - 32\Omega_e^{max^2}\zeta_e + 8(-\Omega_e^{max^8}\zeta_e^2 \\ &-16\Omega_e^{max^6}\zeta_e^4 - 1024\Omega_e^{max^4}\zeta_e^6 - 2\Omega_e^{max^7}\zeta_e \\ &+32\Omega_e^{max^6}\zeta_e^2 - 96\Omega_e^{max^5}\zeta_e^3 - 4096\Omega_e^{max^3}\zeta_e^5 - \Omega_e^{max^6} \\ &+64\Omega_e^{max^5}\zeta_e - 448\Omega_e^{max^4}\zeta_e^2 + 1024\Omega_e^{max^3}\zeta_e^3 \\ &-6144\Omega_e^{max^2}\zeta_e^4 + 32\Omega_e^{max^4} - 672\Omega_e^{max^3}\zeta_e \\ &+3072\Omega_e^{max^2}\zeta_e^2 - 4096\Omega_e^{max}\zeta_e^3 - 304\Omega_e^{max^2} \\ &+3072\Omega_e^{max}\zeta_e - 1024\zeta_e^2 + 1024)^{1/2} - 32\Omega_e^{max})/ \\ &(\Omega_e^{max^5} + 64\Omega_e^{max^3}\zeta_e^2 + 128\Omega_e^{max^2}\zeta_e + 64\Omega_e^{max})\end{aligned} \quad (6)$$

and, for $\varphi_e^n = 0$, $\beta_e^n = 0$ is considered.

Sub-cycling

Sub-cycling is a subdomain decomposition associated with computations at several time intervals. This technique allows a domain to be discretized considering different refinement levels without limiting its explicit time-marching solution to be restricted to its shortest critical time step. This allows greater time-steps values for different subdomains, enabling lower computational costs. Despite allowing greater time-steps values for different subdomains, enabling lower computational costs, sub-cycling must be properly considered, once excessive subdivisions may provide deterioration in both accuracy and efficiency. Here, an automatic algorithm has been developed to improve efficiency without compromising accuracy.

The following algorithm is considered to define the subdomain decomposition: (i) calculate the critical time-steps of all elements, finding the smallest Δt_e of the model (i.e., Δt_b, where $\Delta t_b = \min(\Delta t_e)$), which is the basic time-step for the controlled subdivision of the domain; (ii) with Δt_b defined, calculate subsequent time-step values as multiple of the power of 2 of this minimal time-step value (i.e., calculate Δt_i, where $\Delta t_i = 2^{(i-1)}\Delta t_b$); (iii) associate each element to a computed time-step value (i.e., to Δt_i, where $\Delta t_i \leq \Delta t_e \leq \Delta t_{i+1}$ and i indicates the subdomain of that element); (iv) associate a time-step value (i.e., associate a subdomain) to each degree of freedom of the model considering the lowest time-step value of its surrounding elements.

Once the subdomains of the model are stablished, displacement and velocity values along the boundaries of these subdomains may need to be interpolated. In this work, the following expressions are adopted for these interpolations:

$$\mathbf{U}(\mathrm{t}) = \frac{1}{2\Delta t}\left(\dot{\mathbf{U}}^{\mathrm{n}+1} - \dot{\mathbf{U}}^{\mathrm{n}}\right)t^2 + \dot{\mathbf{U}}^{\mathrm{n}}t + \mathbf{U}^{\mathrm{n}} \tag{7a}$$

$$\dot{\mathbf{U}}(\mathrm{t}) = \frac{1}{\Delta t}\left(\dot{\mathbf{U}}^{\mathrm{n}+1} - \dot{\mathbf{U}}^{\mathrm{n}}\right)t + \dot{\mathbf{U}}^{\mathrm{n}} \tag{7b}$$

where t is the current increment of time ($0 \leq t \leq \Delta t$) for the focused subdomain and Δt is the time-step value of the degree of freedom being interpolated, which is related to another subdomain.

Numerical applications

In this section, two numerical applications are considered, briefly illustrating the performance and potentialities of the discussed techniques. In the first example, the effect of an impulsive load over an infinite domain is studied, whereas, in the second application, a geophysical model is analyzed. The first example is considered here since an analytical solution for this model is available [17], allowing better comparing the results provided by the adopted time-domain solution procedures.

Application 1

In this first example, an infinite elastodynamic model is analyzed, which is subjected to an impulsive load applied in the x direction. Five circular FEM meshes, centered at the applied load point, are employed, taking into account different refinement levels. The number of elements in each adopted mesh are: (i) mesh 1 – 25600 elements; (ii) mesh 2 – 57600 elements; (iii) mesh 3 – 129600 elements; (ix) mesh 4 – 230400 elements; and (v) mesh 5 – 409600 elements.

In Fig.1, time-history results for the horizontal displacements at a point located 1.01 m horizontally away from the applied load are depicted, taking into account several time-marching procedures and the model's analytical response. These results are presented for mesh 2, which is also depicted in the figure (its right half is shown in Fig.1). The convergence curves for these procedures are indicated in the figure as well, depicting the errors of these approaches as mesh refinement is applied. As one can observe, the discussed time-marching procedures provide much more accurate results than standard techniques, and the effectiveness of these novel approaches are improved once subcycling is applied. In fact, as one can notice, the discussed adaptive techniques allow properly dissipating spurious numerical oscillations, providing much better responses than standard dissipative (e.g., the EG-α [8]) or non-dissipative (e.g., the CDM) approaches.

In Tab.1, the performance of each adopted technique is described, taking into account each considered spatial discretization. As one can observe, the α-adap/sub methodology provides the most accurate results, whereas the β-adap/sub approach provides the most efficient analyses (an Intel Core i7 -9750H 2.60GHz processor is considered for the analyses, with multiplications by the element stiffness matrices parallelized with OpenMP using 8 threads).

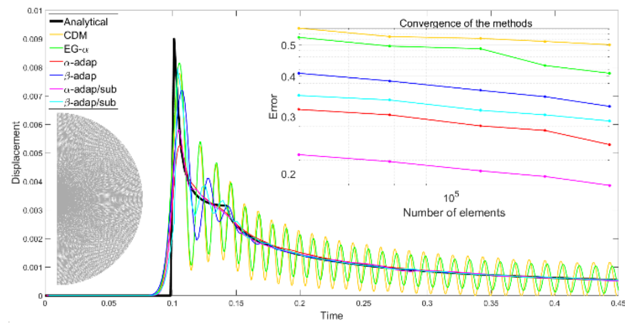

Figure 1 – Time history results for mesh 2 and convergence curves for the discussed time-marching procedures.

Table 1 – Performance of the methods for Application 1

Mesh	Method	Δt $(10^{-2}s)$	Error (10^{-1})	CPU Time (s)
1	CDM	0.12783	5.64	35.270
	EG-α	0.11520	5.28	44.440
	α-adap	0.12783	3.16	34.850
	β-adap	0.26306	4.09	18.540
	α-adap/sub	0.51132*	2.29	9.770
	β-adap/sub	1.05225*	3.49	4.880
2	CDM	0.72227	5.31	143.720
	EG-α	0.65096	4.87	164.220
	α-adap	0.72227	3.04	141.210
	β-adap	1.44455	3.87	66.520
	α-adap/sub	2.88234*	2.18	36.070
	β-adap/sub	5.75470*	3.38	18.740
3	CDM	0.72058	5.24	207.770
	EG-α	0.64944	4.87	217.800
	α-adap	0.72058	2.81	206.690
	β-adap	1.44117	3.62	91.500
	α-adap/sub	2.88234*	2.04	59.310
	β-adap/sub	5.76470*	3.14	27.210
4	CDM	0.56371	5.13	225.520
	EG-α	0.50806	4.32	243.220
	α-adap	0.56371	2.72	224.090
	β-adap	1.12743	3.46	118.760
	α-adap/sub	2.25486*	1.96	70.610
	β-adap/sub	4.50973*	3.04	44.300
5	CDM	0.31077	5.01	791.970
	EG-α	0.28009	4.09	860.460
	α-adap	0.31077	2.46	790.030
	β-adap	0.62155	3.23	445.000
	α-adap/sub	1.24310*	1.84	256.310
	β-adap/sub	2.48621*	2.91	156.120

*Maximal Δt in the multiple time-steps analysis

Application 2

In this second example, the Elastic 2DEW model [18] is analyzed. A sketch of this highly heterogeneous 35 km x 15 km model is presented in Fig.2. A pulse source is applied at the upper surface of the problem, as a vertical load located at $x = 17440m$, and a FEM mesh with 717139 linear triangular elements is adopted for its spatial discretization.

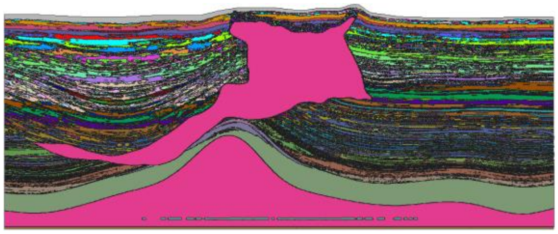

Figure 2: Elastic 2DEW geological model

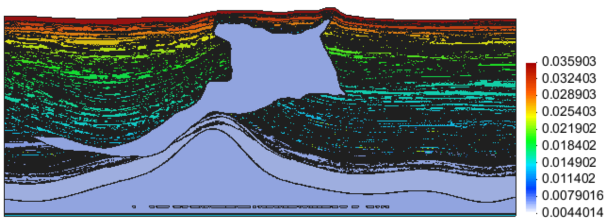

(a)

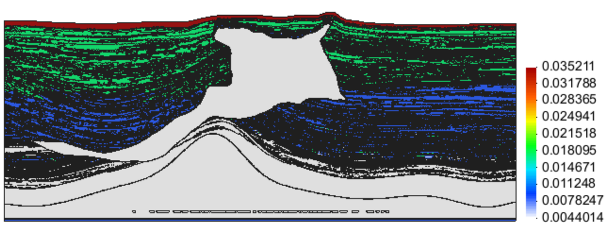

(b)

Figure 3 – Time-step values: (a) per element (intermediate step in the subdivision algorithm); (b) per subdomain for subcycling (final step in the subdivision algorithm).

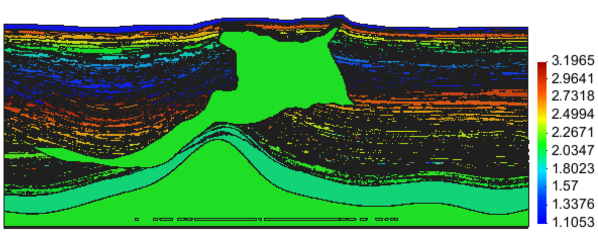

(a)

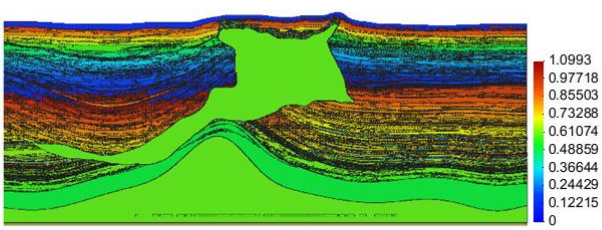

(b)

Figure 4 – Active values of the numerical damping parameters per element: (a) α-adap/sub (α_e^{act}); (b) β-adap/sub (β_e^{act}).

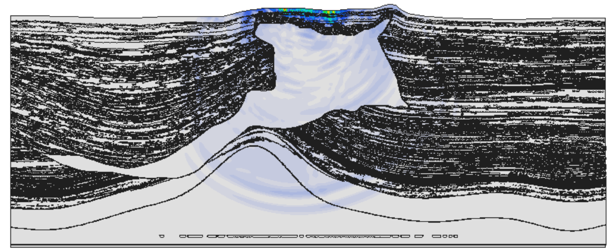

(a)

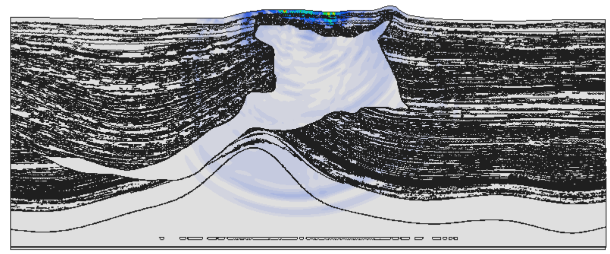

(b)

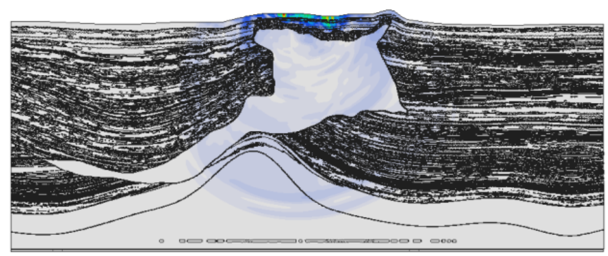

(c)

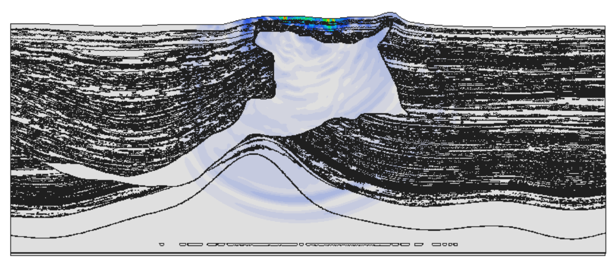

(d)

Figure 5 – Computed results along the discretized domain (t = 20 s): (a) CDM; (b) EG-α; (c) α-adap/sub; (d) β-adap/sub.

Table 2 – Performance of the methods for Application 2

Method	$\Delta t\ (10^{-2}s)$	CPU Time (s)
CDM	0.22069	748.610
EG-α	0.19834	830.460
α-adap/sub	1.76552*	305.970
β-adap/sub	3.53401*	204.230

*Maximal Δt in the multiple time-steps analysis

In this case, the computed time-step value for each element of the model is depicted in Fig.3a, whereas the obtained subdomain division of time-steps for sub-cycling is depicted in Fig.3b. For this configuration, the active parameter values for α and β (eqs.(3) and (6), respectively) are depicted in Figs.4a and 4b, respectively. In Fig.5, the obtained results for the modulus of the computed displacements along the discretized domain, at t = 20 s, is depicted, considering the CDM, the EG-α, the α-adap/sub and the β-adap/sub. In Tab.2 the performance of these techniques are provided.

For this geophysical model, as Fig.5 illustrates, the new methodologies provide similar results to those of standard techniques, although, once again, less spurious oscillations can be perceived in the responses provided by these novel formulations. In addition, as Tab.2 indicates, the efficiencies of the novel procedures are much greater than those of standard approaches, illustrating once again the superior performance of these techniques.

Conclusions

This paper describes two explicit fully-adaptive time-marching formulations for elastodynamic analyses. In these approaches, both time-step and time-integrator values adapt to the properties of the discretized models, allowing to provide more efficient and accurate solution methodologies. In the applications that have been presented in the previous section, the α-adap/sub technique provides the best accuracy among the techniques that are discussed in this work, and the β-adap/sub method provides the lowest computational effort for solution. In fact, as the described examples illustrate, the proposed formulations are very robust and effective to analyze an ample range of complex wave propagation models, describing very attractive methodologies for direct modelling in geophysical applications.

Acknowledgments

The financial support by CNPq (Conselho Nacional de Desenvolvimento Científico e Tecnológico), CAPES (Coordenação de Aperfeiçoamento de Pessoal de Nível Superior), and PETROBRAS (CENPES – 21066) is greatly acknowledged.

References

[1] Soares Jr, D. (2020). A novel time-marching formulation for wave propagation analysis: the adaptive hybrid explicit method. *Computer Methods in Applied Mechanics and Engineering*, *366*, 113095.

[2] Soares Jr, D. (2021). A multi-level explicit time-marching procedure for structural dynamics and wave propagation models. *Computer Methods in Applied Mechanics and Engineering*, 375, 113647.

[3] Zhang, H. M., & Xing, Y. F. (2019). Two novel explicit time integration methods based on displacement-velocity relations for structural dynamics. *Computers & Structures*, 221, 127-141.

[4] Noh, G., & Bathe, K. J. (2013). An explicit time integration scheme for the analysis of wave propagations. *Computers & structures*, *129*, 178-193.

[5] Kim, W. (2019). An accurate two-stage explicit time integration scheme for structural dynamics and various dynamic problems. *International Journal for Numerical Methods in Engineering*, 120(1), 1-28.

[6] Soares Jr, D. (2020). Efficient high-order accurate explicit time-marching procedures for dynamic analyses. *Engineering with Computers*, 1-15.

[7] Soares Jr, D. (2019). An adaptive semi-explicit / explicit time marching technique for nonlinear dynamics. *Computer Methods in Applied Mechanics and Engineering*, 354, 637-662.

[8] Hulbert, G. M., & Chung, J. (1996). Explicit time integration algorithms for structural dynamics with optimal numerical dissipation. *Computer Methods in Applied Mechanics and Engineering*, 137(2), 175-188.

[9] Soares Jr, D. (2019). A model/solution-adaptive explicit-implicit time-marching technique for wave propagation analysis. *International Journal for Numerical Methods in Engineering*, *119*(7), 590-617.

[10] Hilber, H. M., Hughes, T. J., & Taylor, R. L. (1977). Improved numerical dissipation for time integration algorithms in structural dynamics. *Earthquake Engineering & Structural Dynamics*, *5*(3), 283-292.

[11] Wood, W. L., Bossak, M., & Zienkiewicz, O. C. (1980). An alpha modification of Newmark's method. *International journal for numerical methods in engineering*, *15*(10), 1562-1566.

[12] Newmark, N. M. (1959). A method of computation for structural dynamics. *Journal of the engineering mechanics division*, *85*(3), 67-94.

[13] Soares Jr, D. (2015). A simple and effective new family of time marching procedures for dynamics. *Computer Methods in Applied Mechanics and Engineering*, *283*, 1138-1166.

[14] Bathe, K. J., & Baig, M. M. I. (2005). On a composite implicit time integration procedure for nonlinear dynamics. *Computers & Structures*, *83*(31-32), 2513-2524.

[15] Chung, J., & Hulbert, G. M. (1993). A time integration algorithm for structural dynamics with improved numerical dissipation: the generalized-α method. *Journal of Applied Mechanics*, 60(2): 371-375.

[16] Tamma, K. K., Zhou, X., & Sha, D. (2000). The time dimension: a theory towards the evolution, classification, characterization and design of computational algorithms for transient / dynamic applications. *Archives of Computational Methods in Engineering*, *7*(2), 67-290.

[17] Mansur, W. J. (1983). *A time-stepping technique to solve wave propagation problems using the boundary element method* (PhD thesis, University of Southampton).

[18] Fehler, M. (2012). Seam update: Seam phase i rpsea update: Status of simulations. *The Leading Edge*, *31*(12), 1424-1426.